Paper ID APEN-MIT-2019_152
Applied Energy Symposium: MIT A+B
May 22-24, 2019 • Boston, USA

Effective start-up and shutdown strategies for continuously operated biomass torrefaction reactor

Kevin S. Kung
Department of Mechanical Engineering, Department of Biological Engineering, Massachusetts Institute of Technology, USA
kkung@mit.edu

Sonal K. Thengane
Department of Mechanical Engineering, Massachusetts Institute of Technology, USA
sonalt@mit.edu

Ahmed F. Ghoniem
Department of Mechanical Engineering, Massachusetts Institute of Technology, USA
ghoniem@mit.edu

Abstract: In this study, we analyze experimental time series temperature data and infer the transient behaviors of the test reactor, as well as how it changes with reactor scaling. We show that the thermal mass of the reactor has a significant part to play in the reactor's temporal response to changes, and demonstrate that in our design, it is possible to achieve a reasonable temporal response time at scale. Based on our analysis, we devise a series of start-up and cooling operation strategies that seek to optimize the time and feedstock consumption requirements. The insights learned in this study provide a basis for a more comprehensive study of the reactor transitional operations that can be encapsulated into an automated control system to minimize human intervention.

Keywords - start-up, shutdown, torrefaction reactor, transition, biomass

I. INTRODUCTION

The time required to achieve steady state operation is an important factor in biomass conversion reactors, especially at a pilot or higher scales. An unacceptably long start-up time may mean that the output product, for a long while, may not be subject to the correct reaction condition. For biomass torrefaction, longer duration to achieve steady state conditions is an issue of concern and need to be addressed [1]. Most of the laboratory-scale studies on biomass torrefaction have focused on the steady-state operation of the reactor, and so far paid little attention to the practicalities such as starting and shutting down the reactor or adjusting the reaction conditions. Our earlier studies on biomass torrefaction focus primarily on kinetic study [2], reactor design [3], mathematical model [4], and optimizing torrefaction process parameters [5]. The objective of the present work is to analyze experimental data of the laboratory level test reactor and infer the transient behaviors with respect to reactor scaling. We set out to characterize the response time of our laboratory-scale reactor in different modes of operation, such as (a) starting from a cold state, (b) shutting down quickly or slowly. We also derive the scaling laws for this reactor response time, thereby deriving insight into how the response time varies as the reactor size changes. Therefore, we create an analytical framework for characterizing the response time that has applications not only in our laboratory-scale torrefaction reactor, but also more generally to other biomass reactors (e.g. gasifiers, incinerators) as well as beyond.

II. STARTING A REACTOR FROM COLD STATE

The test reactor has an inner radius Rr = 2 inches (5.1 cm) and is comprised of ¼-inch-thick (0.64 cm) stainless steel 304. Then outside of the stainless steel wall, the reactor is surrounded by a formable ceramic insulation sheet that is about 1 inch (2.5 cm) thick. We assume that the reactor is completely filled with biomass (pine shavings, which has a bulk moving bed density of 30 kg m^{-3}). Given these data, we can break down the thermal mass of the reactor into three components: biomass, metal wall, and insulation. Table 1 illustrates calculation of the heat capacity (thermal mass) from these data.

Table 1. Components of thermal mass comprising laboratory-scale reactor assembly.

Components	Biomass (pine shaving)	Metal (SS 304)	Insulation (AlSi)
Volume (cm^3)	49	13	68
Density (kg/m^3)	30	8,050	96
Mass (kg)	0.15	11	0.65
Sp.heat capacity ($J\ K^{-1}\ kg^{-1}$)	1,300	452	1,130
Heat capacity ($J\ K^{-1}$)	190	4,800	740

We first consider the case of starting the reactor from a cold state. Our goal is to identify a start-up strategy that minimizes both the start-up response time and the amount of biomass consumed during the start-up phase. We further assume that we have a specified target temperature T_{target} that the reactor must reach by the end of the start-up phase. First, we remark that during the start-up transition phase, if we are continuously flowing biomass through the system under a small normalized air/fuel ratio $\sigma < 1$—as we would do during the steady-state torrefaction process—then we would waste much of the biomass as it come out unusable due to incomplete torrefaction. Therefore, for the purpose of minimizing wasting biomass, the start-up procedure should bring the normalized air/fuel ratio to stoichiometric combustion ($\sigma \sim 1$). This serves two purposes.

Firstly, it completely combusts the unusable biomass and harnesses all the energy for starting the reactor up; secondly, this method maximizes the flame temperature, thereby heating up the reactor thermal mass more aggressively.

To better understand and quantify the reactor start-up process, we utilized a simplified heat transfer model shown in Fig.1a. Here, at the bottom, the reactor wall is hottest, assuming a temperature T_H. We further estimate that there is some bulk convective transfer coefficient h between the reactor wall and the upflowing post-combustion flue gas, such that when the flue gas escapes from the reactor, it has been cooled to a temperature T_C. Fig.1b shows the corresponding experimental setup. We tested the start-up procedure under two different biomass mass fluxes (which signifies different power outputs for heating up the reactor): 4 g s^{-1} m^{-2}, and 6 g s^{-1} m^{-2}. Note that once the biomass flux was specified, the air flow was adjusted to provide a stoichiometric combustion ($\sigma \sim 1$).

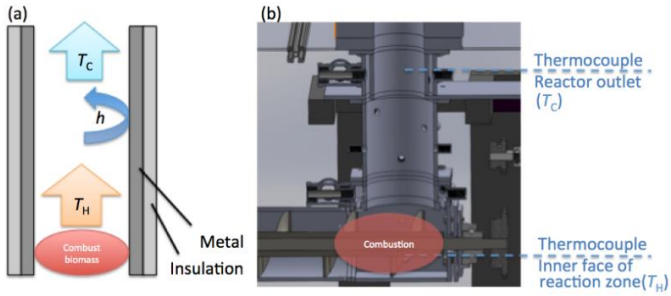

Fig. 1. (a) Conceptual model (b) Experimental setup

Fig.2 shows the temperature traces (in time, where t = 0 represents starting from the cold state) for the lower biomass flux (4 g s^{-1} m^{-2}, Fig.2a) and for the higher biomass flux (6 g s^{-1} m^{-2}, Fig.2b). In both plots, the red line traces the inner surface temperature of the reaction zone (proxy for T_H), and the blue line traces the temperature at the reactor outlet (proxy for T_C). In both cases, the reactor heats up on the order of 2 hours, though depending on the biomass flux (power output), the final steady-state temperature is different: it is around 225 ℃ for a biomass flux of 4 g s^{-1} m^{-2}, and about 290 ℃ for a biomass flux of 6 g s^{-1} m^{-2}.

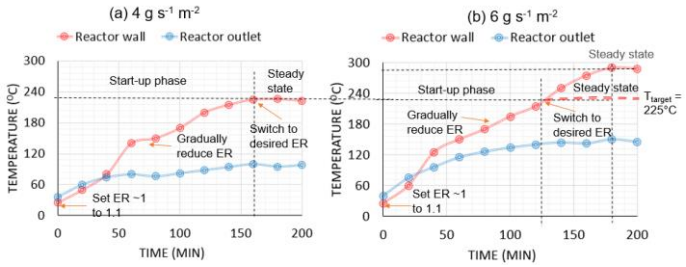

Fig. 2. Temperature traces in time at the inner face of the reaction zone (red lines) and at the reactor outlet (blue)

Given that we know a specific target torrefaction temperature T_{target} to reach, then, firstly, T_{target} sets a constraint on the minimally viable biomass mass flux: as an example, if we want the target torrefaction temperature to be at 260 ℃, then it makes little sense to try to warm up the reactor using a biomass mass flux of 4 g s^{-1} m^{-2}, as we know from the experiment above that under this low flux, the steady-state reactor temperature will never reach 260 ℃. Rather, a higher biomass mass flux is needed. However, as Fig. illustrates, we have various choices for the biomass mass flux: (a) find a biomass mass flux where the final steady-state temperature is just barely above T_{target}, or (b) aim for a higher mass flux with a final steady-state temperature way above T_{target}, and then transition to the continuous steady-state reactor operation as soon as the reactor temperature reaches the vicinity of the target temperature. We see from Fig.3 that these two approaches have a trade-off between the total start-up time required (shorter for scenario b) and the total amount of biomass consumed/wasted for starting the reactor up (lesser for scenario a). We put forth the concept here only, and will work through a more quantitative approach to this design choice/trade-off later in the section.

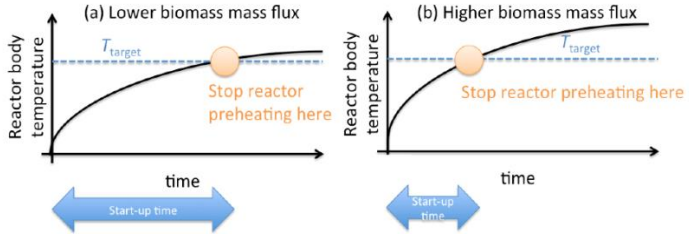

Fig. 3. Trade-off between temperature and time for different biomass mass flux

In order to quantify this trade-off in greater detail, we first need to put some theoretical framework behind the observations above. We first assume that heat transfer from the post-combustion flue gas to the reactor can be approximated as a lump sum. This is true when the Biot number of the reactor assembly is much less than 0.1. We verified that, given the inner metal wall lining with rapid heat conduction, this condition is satisfied. This implies that heating the metal from the post-combustion flue gas—rather than the heat conduction through the metal—is the rate-limiting step in starting up the reactor. The equation below describes that the energy balance of the post-combustion flue gas:

$$\mathcal{E}_{\text{comb}}\dot{m}_{\text{BM}}\text{HHV}_{\text{BM}} = 2\pi R_r L_r h(T_H - T_{\text{metal}}) + \dot{m}_{\text{flue}}c_{\text{p,flue}}(T_C - T_{\text{air}}). \quad (1)$$

Here, the left-hand side represents the heat of biomass combustion (adjusted by a lump-sum efficiency factor $\varepsilon_{\text{comb}} < 1$); the first term on the right-hand side represents the heat transferred from the post-combustion flue gas to the metal body through the convective heat transfer coefficient h, and this process cools the upflowing flue gas from the original T_H at the reactor core to T_C at the reactor outlet; and finally, the second term on the right-hand side represents the sensible heat loss from the warm flue gas at the reactor exit. Here, we do not know

many terms, such as the combustion efficiency factor ε_{comb}, and the specific heat capacity of the flue gas $c_{p,flue}$. But as we will show later, it is not necessary to know the values of these terms in order to approximate the reactor's start-up response time.

Next, we can write the energy balance of the metal as:

$$m_{\text{metal}} c_{\text{metal}} \frac{dT_{\text{metal}}}{dt} = 2\pi R_r L_r h(T_{\text{H}} - T_{\text{metal}}) - \frac{2\pi L_r}{\Omega}(T_{\text{metal}} - T_{\text{air}}), \quad (2)$$

where we have the initial condition $T_{\text{metal}}(t = 0) = T_{\text{air}}$ in the cold state. Here, the first term on the right-hand side represents the heat transfer from the post-combustion flue gas to the metal body, and the second term on the right-hand side represents the heat loss from the metal body through the insulation material to the ambient air, and this loss is governed by the thermal transfer resistance factor Ω, defined as:

$$\Omega \equiv \frac{\ln\left(1+\frac{\Delta_{\text{metal}}}{R_r}\right)}{k_{\text{metal}}} + \frac{\ln\left(1+\frac{\Delta_{\text{ins}}}{R_r+\Delta_{\text{metal}}}\right)}{k_{\text{ins}}} + \frac{1}{h(R_r+\Delta_{\text{metal}}+\Delta_{\text{ins}})} \quad (3)$$

By observing the blue lines in Fig.2, we made the observation that the temperature at the reactor outlet—while fluctuating widely throughout—rapidly assumes its steady-state temperature in comparison with the much slower rise in the reactor core (red lines). Therefore, we can assume that T_{C} is independent of time, and can be represented by some time-independent average value $\langle T_{\text{C}} \rangle$.

By combining the two equations above, and rearranging the terms, we obtain:

$$\frac{dT_{\text{metal}}}{dt} = \frac{\dot{m}_{\text{BM}}}{m_{\text{metal}} c_{\text{p,metal}}}\left(\varepsilon_{\text{comb}} \text{HHV}_{\text{BM}} - \frac{\dot{m} c_{\text{p,flue}}}{\dot{m}_{\text{BM}}}(\langle T_C \rangle - T_{air})\right) - \frac{2\pi L_r}{m_{\text{metal}} c_{\text{p,metal}} \Omega}(T_{\text{metal}} - T_{\text{air}}) \quad (4)$$

Here, if we assume that the heat capacity of the metal does not vary greatly with temperature in our regime of interest,[1] and we assume that $\langle T_{\text{C}} \rangle$ can be approximated as a time-independent constant, then we see that the first term on the right-hand side is approximately a constant term (time-independent), while the second term on the right-hand side has a time-dependent T_{metal} term. For the purpose of curve-fitting from our experimental data, this equation can be simplified into the linear equation $Y = A - X / \tau_s$, where

$$Y \equiv \frac{dT_{\text{metal}}}{dt}, X \equiv T_{\text{metal}} - T_{\text{air}}, \tau_s \equiv \frac{m_{\text{metal}} c_{\text{p,metal}} \Omega}{2\pi L_r} \quad (5)$$

Here, the time constant τ_s in fact represents the response time of the reactor in starting up based on biomass combustion. Table 2 gives the fitting parameters for the two different biomass mass fluxes measured previously.

Table 2. Fitted parameters to calculate the reactor start-up response time.

Biomass mass flux	Fitted value for A	Fitted value for τ_s
4 g s^{-1} m^{-2}	2.10 ± 0.11 [K s^{-1}]	147 ± 1 [min]
6 g s^{-1} m^{-2}	3.15 ± 0.12 [K s^{-1}]	114 ± 1 [min]

Indeed, as remarked earlier, the representative time constant is around 2 hours, which is consistent with our earlier observations. We also see that the fitted constants change as we change the biomass mass fluxes; this should not surprise us, as different temperatures and combustion conditions can affect various factors. We note that the equation contains various reactor's geometrical factors R_{r} and L_{r}, and we can therefore make an educated guess for the new reactor start-up response timescale τ_s^* given new dimensions L_r^* and R_r^* of the scaled-up reactor:

$$\frac{\tau_s^*}{\tau_s} = \frac{L_r^*}{L_r}\frac{\Omega}{\Omega^*} \quad (6)$$

assuming all other factors (such as choice of insulation material) are held constant. By the same logic, we can also make an educated guess for the new reactor start-up response timescale in the lightweight design scenario (where the metal thickness, Δ_{metal}, is 1/16 inches (16 mm) rather than 1/4 inches (64 mm), which also affects the heat transfer resistance term Ω). The results are summarized in Table 3.

We therefore make two observations. Firstly, as we make the reactor lightweight (use less metal), we can drastically reduce the reactor's start-up response time by a factor of 2-3. Secondly, as we scale up the reactor using the current metal thickness (¼-inch stainless steel), the reactor's response time increases only mildly, and therefore, manageably: while the biomass flow rate is increased by a factor of 400 (with 80'' reactor diameter compared to 4'' reactor diameter), for both biomass fluxes, the reactor's start-up response timescale increases only by a factor of 1.3. However, in the case of the lightweight design scenario, as the reactor scales up, the response timescale initially increases mildly, and then decreases at the largest scale (80'' compared to 20'' in reactor diameter) mildly.

Table 3. Predicted reactor start-up timescales under various reactor dimensions and metal thicknesses

		Reactor dimensions (diameter × height)		
Metal thickness	BM mass flux	10 cm × 60 cm	50 cm × 90 cm	2 m × 1.2 m
64 mm (traditional)	4 g s^{-1} m^{-2}	147 min	179 min	188 min
	6 g s^{-1} m^{-2}	114 min	139 min	146 min
16 mm (lightweight)	4 g s^{-1} m^{-2}	52 min	68 min	62 min
	6 g s^{-1} m^{-2}	40 min	52 min	48 min

To intuitively understand this mild dependence as the reactor scales up, we note that in the limit that R_{r} becomes very large in comparison with Δ_{metal} and Δ_{ins}, we can approximate the response timescale as

$$\tau_s = \frac{\pi L_r((R_r+\Delta_{\text{metal}})^2 - R_r^2)c_{\text{p,metal}}\Omega}{2\pi L_r} \longrightarrow \frac{c_{\text{p,metal}}\Delta_{\text{ins}}}{k_{\text{ins}}}\Delta_{\text{metal}}(1+\Delta_{\text{metal}}) \quad (7)$$

The strong dependency on Δ_{metal} explains the drastic improvement in the reactor's response time in the lightweight design scenario, and the fact that this expression has no dependence on the reactor's dimensions explains why the response timescale changes only mildly as the reactor scales up: the timescale is asymptotically approaching a constant value that depends only on the insulation and the metal thickness.

Now, with the reactor's start-up response timescale quantified, we can proceed to capture this trade-off also in a more quantitative manner. For the ease of analysis, we will assume that the target reactor temperature is T_{target} = 225 ℃, and carry out the analysis using the two biomass mass fluxes that we experimentally carried out to measure the temperatures in Fig. . This process below is used as an example to illustrate an experimental and design framework that can be generalized (for other biomass mass fluxes) to optimize the reactor start-up operations for other target temperatures and types of biomass.

If we want to reach T_{target} = 225 ℃ with a biomass mass flux of Φ_{BM} = 4 g s^{-1} m^{-2}, then we see that from Fig. 2a, the red curve takes about τ_t = 130 minutes to cross the 225 ℃ line. This means that for our laboratory-scale reactor with a radius R_r = 2 inches, the total amount of biomass consumed is $m_{\text{BM}} = \pi R_r^2 \Phi_{\text{BM}} \tau_t$ = 252 g. On the other hand, for the biomass mass flux of Φ_{BM} = 6 g s^{-1} m^{-2}, the red curve takes only about τ_t = 95 minutes. In this case, the total amount of biomass consumed is 295 kg. Therefore, we see that in this case, if we put in a higher biomass mass flux, we get a 30% decrease in the overall start-up time, but only a 17% increase in the total amount of biomass consumed/wasted for starting the reactor up. Which mass flux to select depends on the operation needs: if we are in a hurry to process a massive amount of biomass for a long time period, then the time it saves during the start-up phase may very well justify the extra consumption of biomass to start. However, on the other hand, if we are only processing a small batch of biomass, or if the biomass is very expensive, then every gram of it counts, and in this case we may select to have a slower start-up time that also consumes a smaller quantity biomass.

As the reactor scales, we will be processing biomass at a significantly higher flow rate. In order to make the figures comparable between different scales, we define a quantity for the reactor start-up phase called the *specific residence time* τ_r:

$$\tau_r \equiv \frac{\pi R_r^2 \Phi_{\text{BM}} \tau_t}{\dot{m}_{\text{BM}}}, \quad (8)$$

where $\dot{m}_{\text{BM}}$ is the steady-state biomass mass flow rate of the reactor. This quantity has the unit of time. Therefore, in essence, we are normalizing the total biomass consumed/wasted during the start-up period by the nominal steady-state biomass mass flow rate, and this quantity reflects the time's worth of the amount of biomass consumed/wasted during the start-up period. As an example, for the calculations done above for the base case of our laboratory-scale reactor ($\dot{m}_{\text{BM}}$ ~ 0.5 kg h^{-1}). For the case of the lower biomass mass flux, τ_r = 252 g / (500 g h^{-1}) ~ 30 min. For the case of the higher biomass mass flux, τ_r ~ 35 min. Therefore, in terms of the amount of biomass consumed/wasted to warm up the reactor, it represents, respectively, 30 and 35 minutes' worth of continuous reactor processing.

Table 4. Specific residence time for different reactor scales for T_{target} = 225 ℃ for pine shavings.

		Reactor dimensions (diameter × height)		
Metal thickness	BM mass flux	10 cm × 60 cm	50 cm × 90 cm	2 m × 1.2 m
64 mm (traditional)	4 g s^{-1} m^{-2}	30 min	35 min	37 min
	6 g s^{-1} m^{-2}	35 min	42 min	48 min
16 mm (lightweight)	4 g s^{-1} m^{-2}	11 min	13 min	13 min
	6 g s^{-1} m^{-2}	12 min	16 min	15 min

From Table 4 we already observed previously in the reactor response timescale, even as we massively scale up the reactor, the specific residence time is not predicted to change drastically. We assume that for a real-life reactor operation at scale, it will visit a 1-acre farm over a period of one day, processing about 2 dry tons/acre of biomass residues. At a scale of 200 kg h^{-1} (reactor diameter = 80 inches), this requires about 10 hours of continuous operation. Therefore, wasting approximately 40 minutes' worth of biomass to start up the reactor represents no more than 7% of the overall feedstock assuming that the wall is ¼-inch stainless steel. In the lightweight design scenario, the waste represents no more than 3% of the overall feedstock, which is an improvement by more than a factor of 2. This is encouraging, as it suggests that we do not need to implement additional strategies to facilitate the start-up timescale as the reactor scales up.

III. SHUTTING DOWN THE REACTOR

Unlike the case of starting up the reactor, where we tend to want the system response time to be as fast as possible, in the case of shutting down the reactor, the desired system response time depends on the specific use case. For example, in the case of a reactor malfunction, and we want the repair done quickly and safely without affecting the production, then the functional requirement is that the reactor should be cooled down as soon as possible. On the other hand, in the case of finishing the torrefaction reaction at one farm and immediately moving to a different farm, then the functional requirement is that the reactor should stay warm for as long as possible, so that when the unit is moved to the new farm, we do not expend extra energy to try to warm up the reactor assembly again. Due to the limited space in this paper, we will only explore one of the cases here, in cooling the reactor quickly.

A. Cooling the Reactor Quickly

Suppose that the reactor has a fault during operation, and repair needs to be performed quickly and safely in order to minimize reactor downtime. In this case, our interest is in cooling the reactor down as quickly as possible. Instead of filling the reactor with biomass and capping both ends to avoid the natural stack effect, in this case, we want to remove the biomass completely from the inner reactor, and keep the inner metal exposed to the cooling air, such that the reactor body can be cooled both on the inside and the outside (through the outer insulation).

Fig.4a shows the conceptual illustration of this cooling strategy, and Fig. 4b shows the experimental cooling data. On the outside, the air is relatively still (with convective heat transfer coefficient h_s). Inside the reactor, depending on the amount of stack effect and the pressure drive we apply, we can achieve forced cooling to various extents (given by a convective heat transfer coefficient h_f). Here, in our experiment, we let air flow through the reactor at three velocities: 0 cm/s (black), 1.9 cm/s (blue), and 2.8 cm/s (red). The discrete points are real experimental data, while the dashed lines are the exponential curve fits (strategy to be described next) and their error bars.

To develop a quantitative method to curve-fit and extract the quantitative timescale in different cooling scenarios and to infer reactor scaling, we again build a heat loss model based on Fig. 4a by assuming that the reactor body (metal and insulation layers) can be approximated as a simplified lump sum with total mass m_r and specific heat capacity $c_{p,r}$. We can then write the heat loss equation as:

$$m_r c_{p,r} \frac{dT}{dt} = -2\pi L_r \left(h_f R_r + \frac{1}{\Omega_{dr}}\right)(T - T_{air}). \quad (9)$$

Here, the h_f term on the right-hand side represents heat loss due to forced convection inside the reactor, and the Ω_{dr} term on the right-hand side represents heat loss through the reactor's outer insulation:

$$\Omega_{dr} \equiv \frac{\ln\left(1+\frac{\Delta_{metal}}{R_r}\right)}{k_{metal}} + \frac{\ln\left(1+\frac{\Delta_{ins}}{R_r+\Delta_{metal}}\right)}{k_{ins}} + \frac{1}{h(R_r+\Delta_{metal}+\Delta_{ins})}. \quad (10)$$

By assuming that only the temperature T is the time-dependent term, we can then define the rapid cooling reactor response time τ_{dr} as: $\tau_{dr} \equiv \frac{m_r c_{p,r}}{2\pi L_r\left(h_f R_r + \frac{1}{\Omega_{dr}}\right)}$. (11)

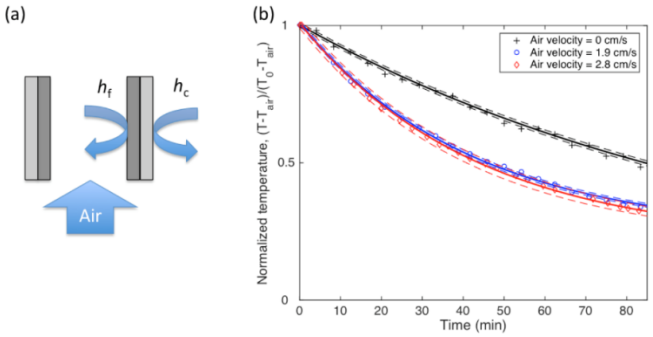

Fig. 4 - Sample temperature trace in time showing the cooling profile for an experiment with pine shavings

By fitting the various experimental data in Fig. 4b with decaying exponentials and then extracting the time constant, we obtained the following time constants: at an air velocity of 0 cm/s, τ_{dr} = (124.1 ± 0.6) min; at 1.9 cm/s, τ_{dr} = (78.1 ±3.7) min; and at 2.8 cm/s, τ_{dr} = (76.7 ±9.2) min. We can therefore see that forced convection does result in faster cooling timescales. For timescale dependence on velocity, we assume that the forced convective heat transfer coefficient, h_f, is a *linear* function of the air velocity:

$$h_f(v_{air}) \approx h_f^0 + \left(\frac{dh_f}{dv_{air}}\right) v_{air}. \quad (11)$$

Then, we can rewrite the rapid cooling timescale equation as:

$$\left(\frac{1}{\tau_{dr}}\right) = \frac{2\pi L_r R_r}{m_r c_{p,r}}\left(\frac{dh_f}{dv_{air}}\right) v_{air} + \frac{2\pi L_r}{m_r c_{p,r}}\left(h_f^0 R_r + \frac{1}{\Omega_{dr}}\right). \quad (12)$$

We can see that this equation is of the linear form $Y = a\,X + b$, where $Y = 1/\tau_{dr}$, and $X = v_{air}$..

Using the same logic of proportionality as described in the previous section, Table 5 reports the outcomes from scaling the reactor up. From Table 5, we observe that as we increase the forced cooling air velocity inside the reactor from 0 to 1.9 cm/s, there is a reduction in rapid cooling time by almost 40%. However, additional velocity increase to 2.8 cm/s only sees a very marginal further reduction. Therefore, we conclude that forced air cooling is effective in moderate velocities. Furthermore, as the reactor scales up, we generally see a weak dependency in the rapid cooling timescale. Finally, as we reduce the metal thickness to 1/16 inches (16 mm), the rapid cooling timescale decreases by a factor of about 3. Therefore, in consideration of rapid cooling, the reactor should be as thermally light as possible. Another alternative strategy for enhancing the rapid cooling of the reactor is to design the outer insulation to be removable. In the case of warming up the reactor as quickly as possible and/or preserving heat within the reactor as long as possible, it is in our interest to put the thermal insulation on the exterior of the reactor. However, in the case of rapidly cooling the reactor, if we are able to remove this external insulation jacket, then this will drastically cut down the Ω_{dr} term, which is also expected to decrease the rapid cooling time even further.

Table 5. The reactor's rapid cooling timescale, for different reactor scales for pine shavings

		Reactor dimensions (diameter × height)		
Metal thickness	Air velocity	10 cm × 60 cm	10 cm × 60 cm	10 cm × 60 cm
1/4 inches or 16 mm (traditional)	0 cm s^{-1}	124 min	115 min	114 min
	1.9 cm s^{-1}	78 min	73 min	72 min
	2.8 cm s^{-1}	77 min	71 min	70 min
1/16 inches or 16 mm (lightweight)	0 cm s^{-1}	41 min	38 min	38 min
	1.9 cm s^{-1}	26 min	24 min	24 min
	2.8 cm s^{-1}	25 min	24 min	23 min

Table 6. A summary of the two cooling modes explored in this study.

	Slow cooling mode	Fast cooling mode
Purpose	Retain heat as long as possible	Lose heat as quickly as possible
Use case	Reactor is being moved from one farm to the next for ongoing conversion.	Reactor breaks down and needs quick and safe service.
Strategy	Fill interior with biomass; cap top and bottom to eliminate stack effect.	Empty biomass, drive forced cooling air through the reactor interior.
Scaling performance	2-3 times improvement in storage time as reactor scales by 400 times	Weak reduction in rapid cooling time as reactor scales by 400 times
Reducing metal use	Adversely affects performance	Improves performance

In the first application, we want to retain as much of the heat for as long as possible. In the second application, we want to cool as rapidly as possible. We showed that with the current reactor design, all these processes happen in the timescale of an hour to hours. However, the two applications have design requirements that are diametrically opposite from each other: the former (slow cooling) requires as much thermal mass and insulation as possible, while the latter (rapid cooling) requires the reactor to be as thermally agile as possible. In each single design, it is not possible to accomplish both optimally. Therefore, the final design will depend on the actual operation requirements, in order to prioritize the design requirements. Another alternative, as discussed earlier, is to design the outer insulation jacket to be removable on demand. While this may increase the complexity and overall capital cost of the reactor, the benefit is a higher performance in both cooling applications. Table 6 summarizes the features of two different cooling modes.

IV. CONCLUSION

We studied the transient timescales of the laboratory-scale reactor assembly and predicted the transition for scale-up reactors. We identified that for rapid warming up and cooling, thermal agility is a desired property of the reactor, and this can be effectively achieved by reducing the amount of metal we use in designing the reactor. Thermal agility can be further improved by designing a removable exterior insulation jacket in the case of the need for rapid cooling. This may seem like a peripheral study as it does not delve into the underlying thermochemistry of torrefaction, but nonetheless it is important from the perspective of understanding how we can most effectively start a reactor from a cold state, and then after a fruitful steady-state production of torrefied output, shut it down effectively or move it elsewhere to operate at a different reaction condition. While adjusting the reactor condition, it may be more time-efficient to utilize the rapid start-up or rapid cooling procedure. Finally, the insights learned in this study will also be helpful towards the design of an automated control system that can achieve these transition goals efficiently. With the few experimental conditions carried out, this study only serves as an initial proof of concept based on which a more extensive set of tests can be carried out for all the imaginable reactor operation and transition conditions.

REFERENCES

[1] Kung KS. Design and Validation of a Decentralized Biomass Torrefaction System. Massachusetts Institute of Technology May, 2017.
[2] Bates RB, Ghoniem AF. Biomass torrefaction: Modeling of volatile and solid product evolution kinetics. Bioresour Technol 2012;124:460–9.
[3] Kung KS, Shanbhogue S, Slocum AH, Ghoniem AF. A decentralized biomass torrefaction reactor concept. Part I: Multi-scale analysis and initial experimental validation. Biomass and Bioenergy 2018:1–8.
[4] Kung KS, Ghoniem AF. A decentralized biomass torrefaction reactor concept. Part II: Mathematical model and scaling law. Biomass and Bioenergy 2018:1–7.
[5] Kung K, Thengane SK, Shanbhogue S, Ghoniem AF. Parametric Analysis of Torrefaction Reactor Operating Under Oxygen-Lean Conditions, Energy 2019;181:603-614